Exp Brain Res (2002) 143:67–77
DOI 10.1007/s00221-001-0970-z

RESEARCH ARTICLE

Charles Capaday

A re-examination of the possibility of controlling the firing rate gain of neurons by balancing excitatory and inhibitory conductances

Received: 18 July 2001 / Accepted: 2 November 2001 / Published online: 21 December 2001

Abstract It has been suggested that balancing excitatory and inhibitory conductance levels can control the firing rate gain of single neurons, defined as the slope of the relation between discharge frequency and excitatory conductance. According to this view the increase in firing rate produced by an input pathway can be controlled independently of the ongoing firing rate by adjusting the mixture of excitatory and inhibitory conductances produced by other pathways converging onto the neuron. These conclusions were derived from a simple RC-neuron model with no active conductances, or firing threshold mechanism. The analysis of that model considered only the subthreshold behaviour and did not consider the relation between total trans-membrane conductance and firing rate. Similar conclusions were also derived from a simple parallel conductance based model. In this paper I consider, as an example of a repetitively firing neuron, a generic model of cat lumbar α-motoneurons with excitatory and inhibitory inputs and a second independent excitatory pathway. The excitatory and inhibitory inputs can be thought of as central descending controls while the second excitatory pathway may represent, for example, the monosynaptic Ia-afferent pathway. I have re-examined the possibility that the firing rate gain of the 'afferent' pathway can be controlled independently of the ongoing firing rate by balancing the excitatory and inhibitory conductances activated by the descending inputs. The steady state firing rate of the model motoneuron increased nearly linearly with the excitatory current, as it does in real motoneurons (primary firing range). The model motoneuron also showed a secondary firing range, whose slope was steeper than in primary range. The firing rate gain was measured by increasing the conductance of the 'afferent' pathway. The firing rate gain (in the primary and secondary firing range) of the 'afferent' pathway was found to be the same regardless of the particular mixture of excitatory and inhibitory conductances acting to produce the ongoing firing rate. This result was obtained for a single-compartment model, as well as for a two-compartment model consisting of an active somatic compartment and a dendritic compartment containing an L-type calcium conductance. Put simply, the firing rate gain of an input to a neuron cannot be controlled by balancing excitatory and inhibitory conductances produced by other independent input pathways, or by the spatial distribution of excitation and inhibition across the neuron. Three potential ways of controlling the firing rate gain are presented in the 'Discussion'. Firing rate gain can be controlled by actions at the presynaptic terminal, by inhibitory feedback, which is a function of the neuron's firing rate, or by neuromodulator substances that affect intrinsic inward or outward currents.

Keywords Membrane conductance · Compartment model · Firing rate · Neuronal gain control · Neuron excitability

C. Capaday (✉)
Department of Anatomy and Physiology, Université Laval, Québec City, Canada
e-mail: charles.capaday@anm.ulaval.ca
Tel.: +1-418-6635747, Fax: +1-418-6638756

C. Capaday
Brain and Movement Laboratory,
Centre de Recherche Université Laval-Robert Giffard,
2601 de la Canardiere, F-6500, Beauport, Québec,
Canada, G1J 2G3

Introduction

In a paper published more than a decade ago, we suggested that the central gain of the monosynaptic component of the stretch reflex could only be controlled by presynaptic inhibition of the Ia-afferent terminals projecting to the α-motoneurons (Capaday and Stein 1987a). The basis of that conclusion was the observation that the reflex output of the motoneuron pool in response to a Ia-afferent input was tied to the background recruitment level (ongoing level of activity) and was independent of the particular mixture of excitatory and inhibitory conductances acting to produce a given recruitment level. In

other words, the size of the reflex response depended only on the strength of synaptic transmission at the Ia-afferent to motoneuron synapses and on the recruitment level of the motoneuron pool. Thus, the gain of this pathway could not be controlled at the postsynaptic level by mixtures of excitatory and inhibitory conductances produced, for example, by descending inputs to the motor pool. We thus suggested that the task dependent changes of the stretch reflex output observed experimentally in tasks such as standing, walking and running (Capaday and Stein 1986, 1987b; Crenna and Frigo 1987) were due to changes of presynaptic inhibition of the Ia afferents (Capaday and Stein 1987a). The predictions of our model were subsequently tested in experiments on decerebrate cats (Capaday and Stein 1989). It was shown that the soleus monosynaptic reflex output was tied to the recruitment level of the motoneuron pool regardless of the combination of excitatory (crossed-extension reflex pathway) and inhibitory inputs (e.g. Renshaw inhibition) acting on the pool (see also Henneman and Mendell 1981). This was ipso facto an explicit statement that the gain of single neurons cannot be controlled by postsynaptic conductance changes, consistent with the intracellular current injection studies of Granit et al. (1966). This idea also implies, explicitly, that shunting inhibition is not divisive as had been generally assumed (see Holt and Koch 1997). Unfortunately, the idea that firing rate gain cannot be controlled by postsynaptic conductance changes has not received wide acceptance and continues to be the basis of many neurophysiological models ranging from electrolocation in weakly electric fish (Nelson 1994) to models of simple cells in area V1 of the cerebral cortex (Carandini and Heeger 1994).

For example, in weakly electric fish there is no mechanism for controlling the sensitivity of the electroreceptor afferents. These afferents synapse directly on E cells of the first sensory relay nucleus. It has been shown that the gain through the first sensory relay nucleus is modified without a significant change of the baseline spontaneous activity of the output E cells of this nucleus (Bastian 1986a, 1986b). Descending excitatory and inhibitory pathways are known to exist on the apical dendritic and somatic regions, respectively (Bastian and Courtright 1991). This is akin to the descending excitatory and inhibitory inputs on spinal motoneurons. The strong conceptual analogy between the gain control of an afferent pathway through the electrosensory relay nucleus of weakly electric fish and the gain control of the Ia-afferent pathway through a mammalian motoneuron nucleus is thus striking. Nelson (1994) suggested that the firing rate gain of E cells was controlled by appropriately balanced levels of excitatory and inhibitory conductances changes produced by descending inputs, such that the background firing rate would not be modified. This is a contradiction of our modelling results on the reflex output of a motoneuron pool (Capaday and Stein 1987a). Although the emphasis of our modelling studies was on understanding population responses, the model was based on a realistic description of single motoneurons and the statistical distribution of intrinsic conductance parameters across the motor pool. Nelson's model was a simple RC-type neuron with no active conductances, or a spike generating mechanism, and the analysis was restricted to subthreshold membrane potential levels. More importantly, the relation between total trans-membrane conductance and discharge rate was not analyzed.

In this paper the balancing of postsynaptic conductances as a mechanism of gain control is tested more fully by considering: (1) the steady state and transient firing behaviour of neurons, (2) the effects on non-linear frequency vs current curves and (3) the spatial distribution of excitatory and inhibitory inputs on a neuron.

Materials and methods

Description of the model

The basic physiological properties of spinal α-motoneurons and the parameter space needed to produce a model of this neuron are well characterized (e.g. Heckman 1994; Granit 1972; Powers 1993). Thus, a realistic α-motoneuron model (Capaday and Stein 1987a; Powers 1993) was used as an example of a generic repetitively firing neuron. The purpose of this study was not to produce a state of the art model of α-motoneurons, but simply to use a physiologically plausible yet computationally tractable neuron model sufficient to explore the issues at hand (e.g. see Matthews 1999). Figure 1A schematically illustrates the neural circuit which was simulated. Descending excitatory and inhibitory inputs to the neuron determine its ongoing firing rate; the added excitation produced by the afferent input will lead to an increase in the firing rate. The main idea pursued in these simulations was to determine the relation between firing rate and excitatory conductance. The slope of this relationship represents the sensitivity, or firing rate gain, of the neuron to an excitatory input. The question posed was whether the firing rate gain of the independent afferent input to the motoneuron changes, depending on the mixture of descending excitatory and inhibitory conductances underlying the ongoing firing.

The results presented herein are derived from a spatially homogeneous motoneuron model and a two-compartment model, each based on time and voltage dependent ionic conductances. The spatially homogeneous model was not chosen because of its relative simplicity. Rather, it was specifically chosen because any conductance change has maximal effects on the dynamics of the neuron (i.e. there is no attenuation of conductance changes). The two-compartment model includes a dendritic compartment with an L-type calcium conductance electrically coupled to an active somatic compartment. In this model changes in the dendritic conductance are readily detected in the soma and vice versa. Again the point was to insure that conductance changes made to any part of the 'neuron' have strong effects on the dynamics. A second reason for adopting a two-compartment model was to determine whether the site at which conductances are changed has an effect on firing rate gain. A third reason for choosing a two-compartment model was to keep the number of possible combinations of excitation and inhibition tractable. In this model there are already nine possible ways to distribute excitation and inhibition across the 'neuron'.

Computational procedures

The values of the somatic conductances and time constants were taken from the extensive simulations of cat α-motoneurons done by Powers (1993); they are presented along with other simulation parameters in Table 1. The motoneuron model used in the present simulations is closely related to the one used in our previous

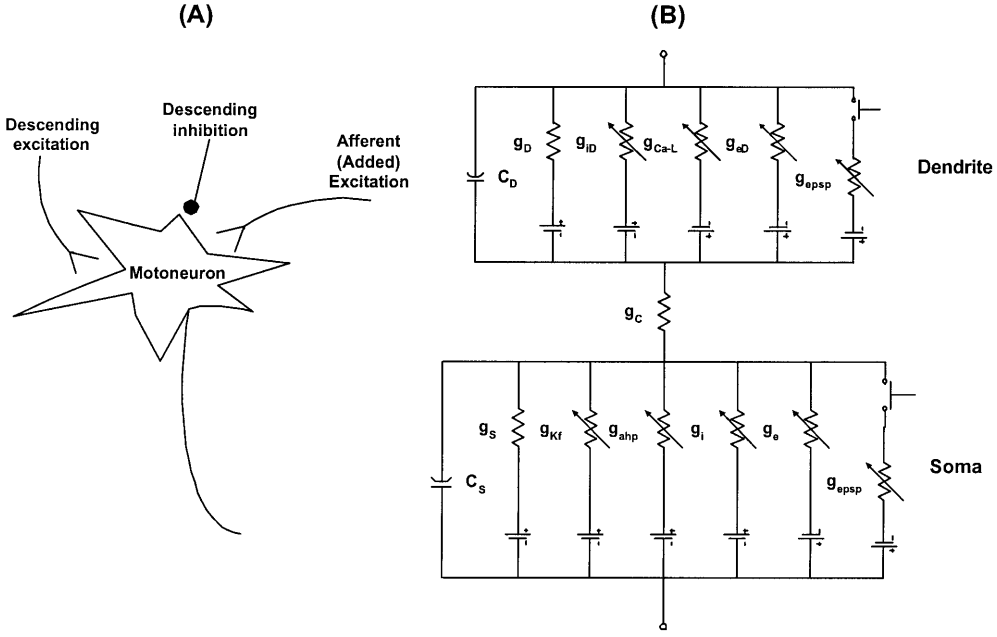

Fig. 1 A schematic representation of the neural circuit investigated in the present simulations is shown in **A**. The equivalent electrical circuit of the two-compartment α-motoneuron model used in the present simulation study is shown in **B**

Table 1 Parameter values, or range, used in the computations. These parameters would be those of a typical motoneuron with an input resistance of 1 MΩ and a resting membrane time constant of 6 ms. Other parameter values are given in the text

Parameter	1-C value(s)	2-C value(s)
Membrane capacitance (C_s, C_D)	6 nF	0.55, 5.46 nF
Resting conductance (g_s, g_p)	1 µS	0.1, 0.45 µS
Threshold (*Vt*)	10 mV	10 mV
Resting and excitatory reversal potential (*Vr*, *Ve*)	0, 50 mV	0, 50 mV
Inhibitory and potassium reversal potential (*Vi*, *Vk*)	–10, –15 mV	–10, –15 mV
Fast potassium conductance (g_{kf})	0.7–1 µS	0.7–1 µS
Afterhyperpolarization conductance (g_{ahp})	2.8 µS	2.8 µS
Decay time constant of g_{Kf}	3–4 ms	3–4 ms
Decay time constant of g_{ahp}	18–22 ms	18–22 ms

study (Capaday and Stein 1987a) of the input-output properties of motoneuron pools and is essentially similar to one of the motoneuron models dealt with by Powers (1993), his '*two time-dependent potassium conductances and fixed spike threshold*' model. For the two-compartment model the dendritic compartment was electrically coupled to the soma such that the ratio of dendritic to somatic conductance was about ten. The electrical equivalent diagram of the motoneuron model is presented in Fig. 1B. The model includes resting somatic (g_S) and dendritic conductances (g_D) and excitatory (g_{eS}, g_{eD}) and inhibitory ($g_{iS,}$ g_{iD}) conductances, which represent, in effect, descending excitation and inhibition as shown in Fig. 1A. The somatic and dendritic excitatory and inhibitory conductances were independently controlled. When the spike threshold is reached – fixed at 10 mV more depolarized than the resting membrane potential (*Vr*), set to zero – the membrane potential is set to 90 mV for 1 ms, thus simulating the occurrence of a spike (Powers 1993). It is important to note that the time of occurrence of spikes is explicitly computed in the simulations, from which the firing rate can be calculated and more importantly the ratio of frequency (*F*) to excitatory conductance. This is akin to the classic frequency/current (*F/I*) relation developed by Granit et al. (1966) and represents, in the formal sense, the firing rate gain of a neuron (or more correctly the firing rate sensitivity, since this ratio is not dimensionless). Following the occurrence of a spike, a fast potassium conductance g_{Kf} at the soma quickly repolarizes the motoneuron (Barrett et al. 1980), whereas the slower calcium dependent afterhyperpolarization (AHP) conductance (g_{ahp}) regulates the firing rate (Granit 1972; McCormick 1990). The following pair of coupled differential equations gives the rate of change of membrane potential in each compartment:

$$C_D\frac{dV_D}{dt} = g_D(Vr-V)+g_{eD}(Ve-V)+g_{iD}(Vi-V) +g_{epspD}(Ve-V)+g_C(V_S-V_D) \quad (1)$$

$$C_S\frac{dV_S}{dt} = g_S(Vr-V)+g_{eS}(Ve-V)+g_{iS}(Vi-V) +g_{Kf}(Vk-V)+g_{aph}(Vk-V) +g_{epspS}(Ve-V)+g_C(V_D-V_S) \quad (2)$$

This coupled pair of equations is non-linear and has no analytical solution. Therefore, the time dependence of the membrane potential was obtained by numerical integration of the equations with respect to time. The non-linearity is due to the product of the time dependent AHP conductance with the membrane potential and more generally any of the conductances may be non-linear functions of time or membrane potential. The computational procedures essentially followed the scheme developed by MacGregor (1987) and commonly used in single neuron modelling (e.g. Powers 1993) and physiological neural network models (e.g. Xing and Gerstein 1996). By setting the coupling conductance g_c to zero and appropriately scaling the membrane capacitance and resting conductance, Eq. 2 reduces to a description of a single-compartment model.

An L-like calcium conductance ($g_{Ca\text{-}L}$) is thought to be located in the dendrites of α-motoneurons (Bennett et al. 1998; Hounsgaard and Kiehn 1993; Lee and Heckman 1996). This conductance contributes a net inward current that underlies bistable firing behaviour (e.g. see Kiehn 1991). Following the work of Booth et al.

(1997), an L-type calcium conductance was introduced in the dendritic compartment. The time constant of activation of this conductance was set at 40 ms (Booth et al. 1997). The conductance had a steep voltage dependent activation (half activation dendritic potential = 15 mV) and a peak conductance of 0.18 μS (Booth et al. 1997; Powers 1993).

A two-step process is required to obtain the steady state somatic (V_S) and dendritic (V_D) membrane potentials, respectively. First, the steady state membrane potential is calculated for each compartment assuming the other compartment is coupled to it but passive, thus:

$$V'_S = \frac{(g_{eS} \times Ve + g_{iS} \times V_i + g_S \times Vr)}{(g_{eS} + g_{iS} + g_S + g_{Deq})} \tag{3}$$

$$V'_D = \frac{(g_{eD} \times Ve + g_{iD} \times V_i + g_D \times Vr)}{(g_{eD} + g_{iD} + g_D + g_{Seq})} \tag{4}$$

The equivalent conductance of the dendritic compartment coupled to the soma (g_{Deq}) and, conversely, of the somatic compartment coupled to the dendrites (g_{Seq}) is given by:

$$g_{Deq} = \frac{g_C \times g'_D}{g_C + g'_D} \quad where,\ g'_D = g_D + g_{eD} + g_{iD} \tag{5}$$

$$g_{Seq} = \frac{g_C \times g'_S}{g_C + g'_S} \quad where,\ g'_S = g_S + g_{eS} + g_{iS} \tag{6}$$

From the above sets of equations (Eqs. 3–6), the steady state somatic and dendritic potentials for the general case where both compartments are simultaneously active are given by:

$$V_S = \frac{g_C \times V'_D}{g_C + g'_S} + V'_S \tag{7}$$

$$V_D = \frac{g_C \times V'_S}{g_C + g'_D} + V'_D \tag{8}$$

The relation of the somatic (V_S) to dendritic (V_D) steady-state potential is obtained by application of the voltage divider principle, thus:

$$V_S = \frac{g_C}{g_C + g'_S} \times V_D = K_{D,S} \times V_D \tag{9}$$

$$V_D = \frac{g_C}{g_C + g'_D} \times V_S = K_{S,D} \times V_S \tag{10}$$

These two equations are important for calculating the steady-state attenuation of voltage from the dendritic to the somatic compartment ($K_{D,S}$) and vice versa ($K_{S,D}$). They are also useful for evaluating the current attenuation from the dendritic to the somatic compartment (and vice versa) when the latter is at a given potential (e.g. 'voltage clamped'). Under this condition the current attenuation factor from dendrite to soma is $K_{S,D}$ and from soma to dendrite $K_{D,S}$ (Johnson and Wu 1995).

Repetitive firing was produced by a step change of the excitatory conductance, at the soma (g_{eS}) or at the dendrites (g_{eD}), or both. Repetitive firing could also be produced by a step change of the excitatory conductances as well as a step change of the inhibitory conductances (g_{iS}, g_{iD}); the total membrane conductance would thus be increased when the two pathways are simultaneously active. A second independently controllable excitatory input is included in the model (Fig. 1A). It represents the added excitatory drive produced by a second input pathway to the neuron, such as the monosynaptic inputs from group Ia afferents. In Eqs. 1 and 2 this second excitatory input is represented by an excitatory postsynaptic potential (EPSP) conductance (g_{epsp}), whose time course is often calculated from the alpha function (Jack et al. 1975). However, in the present simulations a step change of the EPSP conductance was used, simulating a tonically active afferent input. The analysis of transient EPSP inputs has been dealt with in a previous paper (Capaday and Stein 1987a). Obviously, when the inhibitory conductance is increased in any compartment the firing rate will be reduced if the excitatory input is kept constant. However, the firing rate can be maintained at the same level by increasing the excitatory conductance. The general principle involved in deriving the equation for compensating for the added inhibition is the following. The excitatory current must be increased by an amount that is equal and opposite to the inhibitory current (Capaday and Stein 1987a). In the general case, however, the excitatory current can be increased in any compartment. This implies that the current attenuation from one compartment to the other must be also taken into account. From these principles it can be shown that the change in excitatory conductance needed to compensate for the inhibitory conductance is given by the following equation:

$$\Delta g_{e,y} = \frac{(Vt_x - Vi)}{(Ve - Vt_y)} \times \Delta g_{i,x} \times \frac{K_{S,x}}{K_{S,y}} \tag{11}$$

where Vt_x and Vt_y are the membrane potentials in compartment x and y, respectively, when the soma is at spike threshold (Vt_s). This equation is applicable to the case where Vt_s is fixed, which is the case in the present model. Vt_x and Vt_y can be calculated from Eqs. 7 and 8. Equation 11 states that the amount ($\Delta g_{e,y}$) by which the excitatory conductance in compartment y (a nominal variable, y = either s or d) needs to be increased is a proportion of the increase ($\Delta g_{i,x}$) of the inhibitory conductance in compartment x (a nominal variable, x = either s or d) scaled by the ratio of the current attenuation factors ($K_{S,x}/K_{S,y}$). It can be easily verified from Eq. 11 that, at spike threshold in the soma, the added excitatory current will be equal and opposite to the inhibitory current, with each current scaled by the appropriate current attenuation factor.

All numerical calculations were done with Mathcad 2000 and graphical display of simulation outputs with Matlab 5.3.

Results

The time course of the membrane potential (Vm) during several discharge cycles of the single-compartment α-motoneuron model is shown in Fig. 2. Repetitive discharge was produced by two different combinations of excitatory and inhibitory conductances producing a steady-state discharge rate of 19.2 impulses/s (Imp/s). An excitatory conductance of 0.46 μS acting alone produces an interspike interval (ISI) of 50.2 ms or, equivalently, a firing rate of 19.2 Imp/s. If, for example, a tonic level of inhibition of 0.2 μS is added, the firing rate decreases to 15.6 Imp/s (ISI = 64.2 ms). To compensate for the effects of the added tonic inhibitory conductance, according to Eq. 11 an increase in the excitatory conductance of 0.1 μS is required to restore the firing rate to 19.2 Imp/s. As can be seen in Fig. 2, regardless of the particular mixture of active excitatory and inhibitory conductances, the time course of the membrane potential and thus the firing rate are essentially identical. This is entirely in agreement with the classic intracellular recording and current injection studies of Granit et al. (1966) and Schwindt and Calvin (1973). However, the question at hand is whether the firing rate gain – defined as the slope of the relation between firing rate and excitatory conductance, or injected current in the work of Granit et al. (1966) – is dependent on the mixture excitatory and inhibitory conductances acting to produce a given firing rate? The results presented in Fig. 3 address this question.

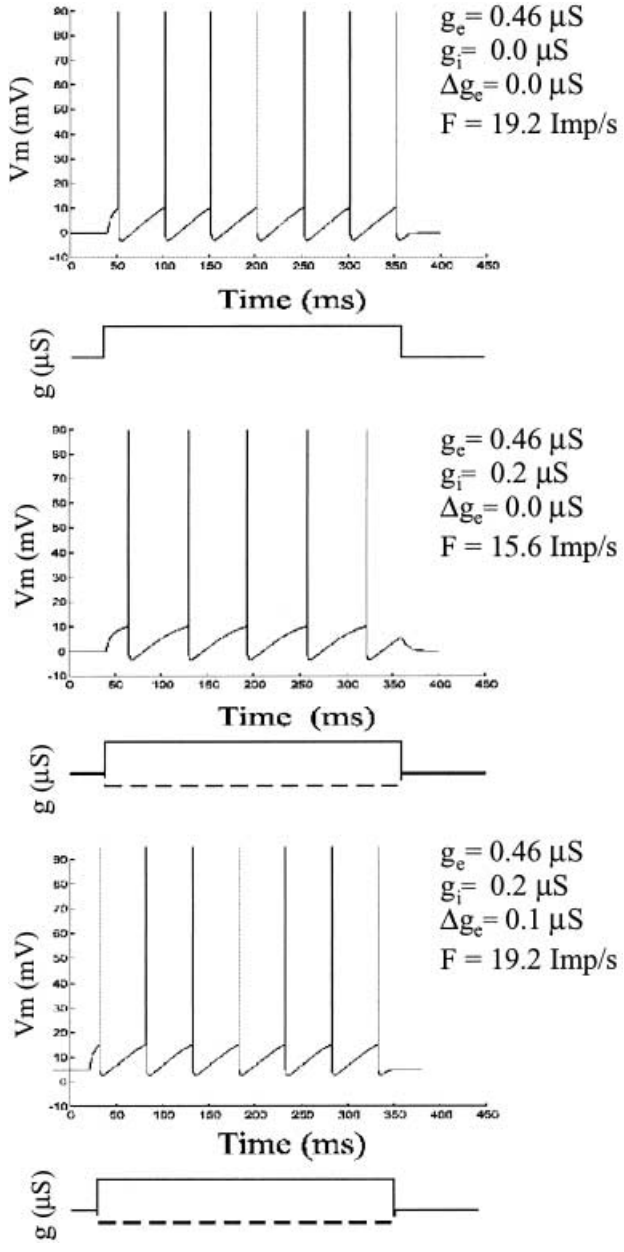

Fig. 2 Steady-state (adapted) repetitive discharge produced by tonic levels of excitatory conductance (g_e) acting alone (*top*), or in combination with a tonic level of inhibitory conductance (g_i) 0.2 µS (*middle and lower*). Note that when the inhibitory conductance is increased, the firing rate (F) is obviously reduced (*middle*). However, when the excitatory conductance is increased by an amount Δg_e=0.1 µS, as calculated from Eq. 11, the firing rate is restored to its initial value (*bottom*)

Consideration of the primary firing range

For the two models considered here the relation between firing rate and excitatory conductance is linear over a substantial portion of the firing range (Fig. 3A, C), as it is for real motoneurons (Granit 1972). The firing rate gain in this 'primary range' was calculated as the slope of the best fitting least-mean-square line, so as to make the simulation results readily comparable to experimental results. In Fig. 3A firing of the single-compartment model was produced by activating the excitatory conductance only, the firing rate gain (F/g_e) being 49.1 Imp/µS. This corresponds to a typical cat lumbar α-motoneuron having an *F/I* slope in the primary range of firing of about 1.0 Imp/nA (Granit 1972). In Fig. 3B a tonic inhibitory conductance of 0.2 µS was added. In order to obtain firing rates over the same range as in Fig. 3A, the excitatory conductance was increased by a constant amount of 0.1 µS, as determined by Eq. 11. Note that the relation between firing rate and excitatory conductance is essentially identical (49.08 Imp/µS), except that it is displaced by 0.1 µS along the abscissa. This result, on its own, makes the point that the firing rate gain is independent of the particular mixture of excitatory and inhibitory conductances – and hence the total membrane conductance – underlying the firing. The same sort of result is obtained with the two-compartment model (Fig. 3C, D). The firing rate gain for the two-compartment model was 52.6 Imp/µS. The slightly greater gain for the two-compartment model is the result of shunting of the AHP current to the dendritic compartment.

The added effect of a second active excitatory pathway is equivalent to increasing the excitatory conductance by a constant amount Δg_e. It is obvious, given the nearly linear relation between firing rate and excitatory conductance, that this will simply shift the F/g_e relation upward by a constant, without a change of slope (Fig. 3). Indeed, for the single-compartment model the *y*-intercept increased by 8.6 Imp/s and 4.2 Imp/s for the two-compartment model. In other words, the firing rate gain is the same for all input pathways to a neuron and it is independent of the particular mixture of excitatory and inhibitory conductances underlying the firing. The firing rate gain is also independent of the distribution of excitatory and inhibitory conductances across the neuron. This point will be dealt with in more detail in the section on the secondary firing range. Note that the increase in firing is greater for the single-compartment (8.6 Imp/s) than for the two-compartment model (4.2 Imp/s). Again, this is because the dendritic compartment shunts part of the added excitatory current.

Transient firing

The analysis thus far dealt with steady-state firing behaviour. Clearly, many neural operations are transient in nature. The question thus arises as to whether the above principle applies to the situation where the input from the second excitatory pathway is phasic (e.g. during a burst of activity). The results shown in Fig. 4 address this point from the perspective of the adaptation of firing rate, which is equivalent to the effects of a transient input. It is well known that upon application of a steady depolarizing current neurons fire initially at a relatively high rate, which then adapts over several interspike intervals to a steady state rate. In the present models, adaptation is due to summation to a maximal value of the

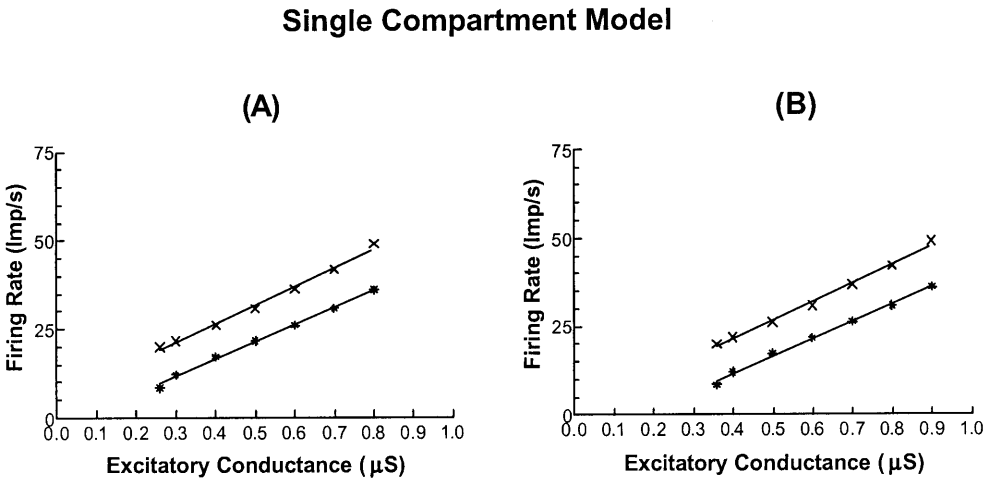

Fig. 3A–D *The lines labeled with asterisks* represent the relation between steady-state discharge rate and excitatory conductance for the single- and two-compartment models. In the graphs shown in **A–D** of the figure *the points marked by* × represent the change in firing resulting from an added afferent input producing an excitatory conductance (Δg_e) of 0.1 µS. Note that the points are all plotted against the value of the excitatory conductance produced by the descending pathway, to emphasize that the effects of the afferent pathway are simply to produce an upward bias of the F/g_e relation, without affecting its slope. For the two-compartment model the excitatory inputs were all localized at the soma. Note also that the same added afferent input (Δg_e) is less effective in increasing the discharge rate of the two-compartment model. In **C** and **D** a tonic inhibitory conductance of 0.2 µS was added. Inhibition simply shifted the F/g_e relations to the right, without affecting their slope

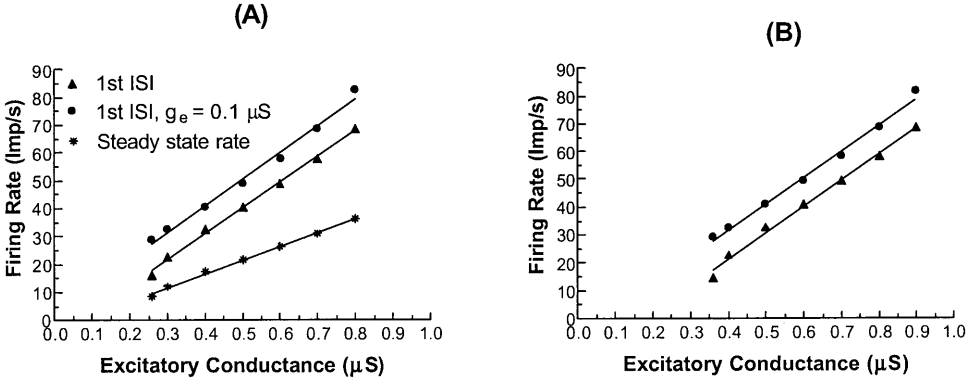

Fig. 4A, B This figure considers the transient firing of the single-compartment α-motoneuron model. In the graph shown in **A** the slope of the relation between the firing rate in the first interspike interval (*1st ISI*) and the excitatory conductance is much steeper than the steady state relation (92.9 Imp/s/µS vs 49.1 Imp/s/µS). In the graphs shown in **A** and **B** of the figure *the points marked by filled circles* represent the 1st ISI resulting from an added afferent input (g_e) producing an excitatory conductance of 0.1 µS. Note that the points are all plotted against the value of the excitatory conductance produced by the descending pathway, to emphasize that the effects of the afferent pathway are simply to produce an upward bias of the transient F/g_e relation, without affecting its slope. In **B** a tonic inhibitory conductance (g_i) of 0.2 µS was added, but the slope of the transient F/g_e relations remains the same

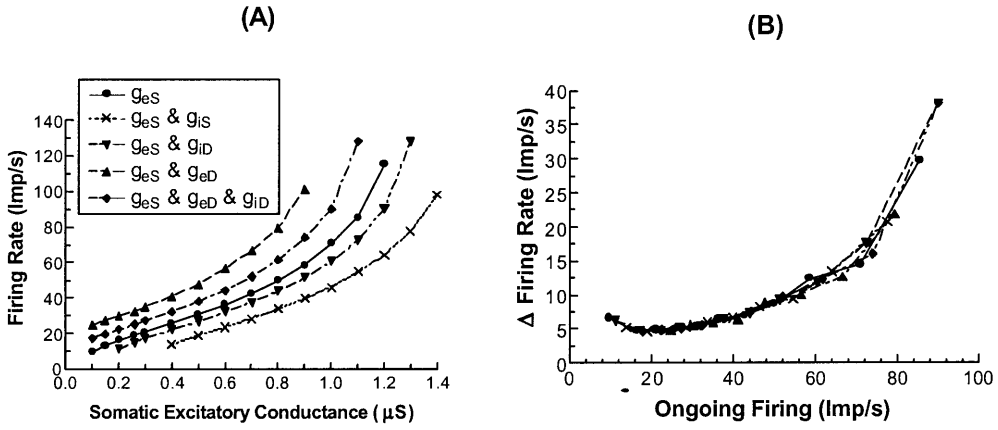

Fig. 5 Examples of F/g_e curves over a full range of depolarizing drive for various combinations and spatial distributions of excitation and inhibition across the two-compartment model **(A)**. For example, simultaneous somatic excitation and inhibition is represented by g_{eS} and g_{iS}, etc., in the legend. Note the obvious secondary range of firing (steepening of the F/g_e relation). Note also that the change of firing rate versus the ongoing firing rate (i.e. a measure of firing rate gain) is the same regardless of the mixture of postsynaptic conductances acting on the neuron, or their spatial distribution

AHP conductance following each spike. Real motoneurons also adapt their firing rate due to an increase in the firing threshold (Schwindt and Calvin 1972a), which can be incorporated into a more complete motoneuron model (Powers 1993). Following the analysis of Kernel (1965), the instantaneous firing rate over the first interspike interval (1st ISI) was used to illustrate transient behaviour. The slope of the F/g_e relation for the 1st ISI is much steeper than the steady-state slope (Fig. 4A), as it is in real motoneurons. Does the slope of the 1st ISI, or that of any other ISI during the firing transient, depend on the mixture of active excitatory and inhibitory conductances? The answer is shown in Fig. 4B, where a constant inhibitory conductance of 0.2 µS was added and the excitatory conductance increased by 0.1 µS, as determined from Eq. 11. Hence, relative to Fig. 4A, the lines are displaced to the right along the abscissa by 0.1 µS. The important point is that, similarly to the slope of the steady-state relation, the slope of the transient F/G_e relation is essentially the same in the two conditions (92.9 Imp/s/µS vs 95.1 Imp/s/µS). The conclusion is that balanced mixtures of excitatory and inhibitory conductances do not affect the firing produced by a transient burst of activity of the second pathway. The transient change in firing rate remains the same, regardless of the mixture of excitatory and inhibitory conductances producing the ongoing firing (Fig. 4B).

Finally, the results presented above apply equally to the case when the inhibitory reversal potential is the same as the resting potential (i.e. shunting inhibition), or when it is more negative (see also Holt and Koch 1997).

Consideration of the secondary firing range

The single-compartment and the two-compartment models show a secondary firing range when driven by intense depolarizing drives (Fig. 5A). An interesting ancillary observation was made by considering either the F/g_e relation (i.e. firing produced by conductance changes) or the F/I relation (i.e. firing produced by current injection) with the firing rate normalized by the reciprocal of the slow AHP time constant. It was found that the upward curvature of the curves begins nearly exactly at the point where the duration of the ISI becomes equal to that of the slow AHP time constant. Thus in the model the secondary firing range arises partly as a result of 'saturation' of the slow AHP conductance (but see the next section).

The more important issue here is whether mixtures of postsynaptic conductances allow for control of firing rate gain when the F/g_e curves are non-linear. The F/g_e curves for five different combinations of excitatory and inhibitory conductances are shown in Fig. 5A. These combinations were chosen for their physiological pertinence, as for example the case of joint somatic and dendritic excitation with inhibition at the soma. For the most part the curves are translated along the abscissa, with little change in their shape. There are, however, some cases were the steepness of F/g_e curve is changed. The clearest example is the effect of dendritic excitation added to somatic excitation (g_{eS} and g_{eD} in Fig. 5A). The F/g_e curve appears steeper when the dendritic excitation is added to somatic excitation, as has been previously reported in motoneurons (e.g. Shapovalov 1972). However, there is a problem in reporting data in this way. The x-axis in Fig. 5A represents the somatic current, but not the total current acting at the spike generating zone. Similarly, in the report of Shapovalov (1972), the x-axis represented injected current at the soma, but the total current acting at the spike initiation zone included dendritic currents activated synaptically, as well as the intracellularly injected somatic current. As a result the relation between firing rate and excitation is made to appear steeper than it is. A formally correct and intuitive way of determining whether the firing gain is changed by mixtures of conductances, or by strategic placement of conductances across the neuron, is

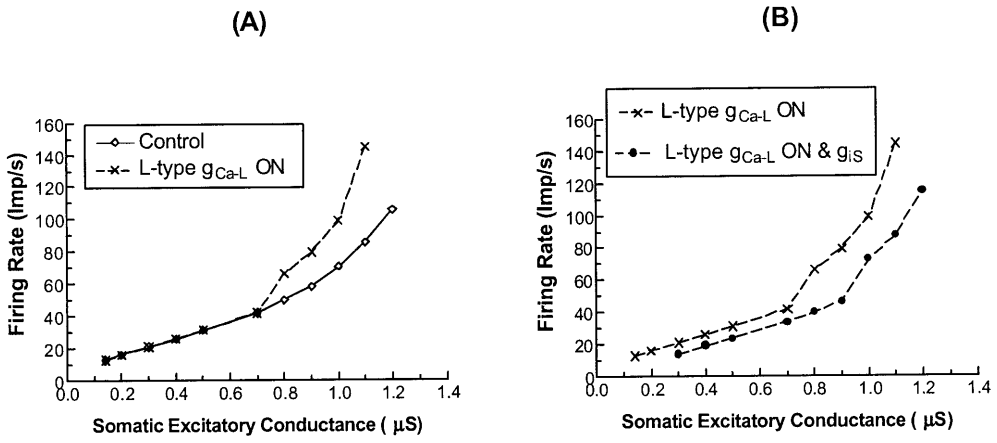

Fig. 6A, B Effects of activating an L-type calcium conductance in the dendrites on the F/g_e curve of the two-compartment model. **A** Note the steeper (1.74 times) secondary firing range, starting at about 40 Imp/s, when the L-type calcium conductance is activated. **B** In the presence of an activated L-like calcium conductance, the addition of somatic inhibition (0.3 µS) translated the F/g_e curve to the right without affecting its shape. Note also that in the presence of inhibition the L-type calcium conductance was activated at a slightly higher firing rate. The same qualitative result is obtained by distributing inhibition to the dendritic as well as the somatic compartment

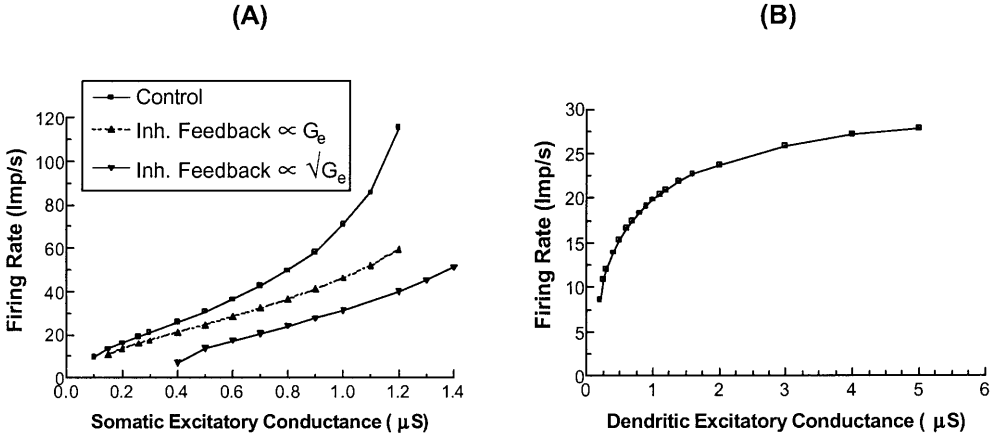

Fig. 7 The effects of inhibitory feedback on the F/g_e relation of the two-compartment model are shown in **A**. In this example the excitatory and inhibitory conductances were all localized to the somatic compartment. Note the obvious secondary range of firing (steepening of the F/g_e relation) under control conditions. Note also how inhibitory feedback extends the linear range of the F/g_e relation. **B** shows an example of the F/g_e relation when the excitatory conductance (g_{eD}) is localized entirely to the dendritic compartment

to plot the change of firing rate as a function of the ongoing firing rate, as shown in Fig. 5B. It can be seen that in fact firing rate gain is not really different for any of the combinations of excitation and inhibition, or for different spatial locations of these variables.

L-like calcium conductance activation and the secondary firing range

Activation of the L-like calcium conductance leads to a persistent inward dendritic current and a steepening of the F/g_e current (Fig. 6A). This is as expected and consistent with one of the functional roles of this persistent current (Schwindt and Crill 1982). Activation of the persistent inward calcium current resulted in a secondary range whose slope was about 1.74 times steeper than when the dendritic compartment was passive (Fig. 6A). However, despite the fact that the F/g_e relation is nonlinear and that the voltage dependent activation of the persistent inward current is itself a non-linearity, activation of inhibitory conductances did not noticeably change the shape of the F/g_e relation (Fig. 6B). Note also that in the presence of inhibition activation of the L-type calcium current occurred at a slightly higher firing rate.

Feedforward versus feedback inhibition

The added inhibition so far dealt with is of the feedforward type. That is, it is not a function of the firing rate of the neuron. What if the added inhibition were a function of the firing rate of the neuron? This would be true inhibitory feedback. As expected from the basic property of a closed loop negative feedback, the firing rate gain of the neuron is decreased (Fig. 7A). In this example, inhibitory feedback was made either directly proportional to

the excitatory conductance, hence directly proportional to the firing rate, or directly proportional to the square root of the excitatory conductance, hence a non-linear function of firing rate. Inhibitory feedback in each case extends the linear range of the F/g_e relation. In no case could the feedback produce a more curvilinear relation than the control curve. However, a particularly striking observation using the two-compartment model was that the relation between firing rate and dendritic excitation is markedly non-linear (Fig. 7B). This is because of the strong and non-linear attenuation of current as it flows from the dendritic to the somatic compartment. In any case, this shows that a non-linear F/g_e relation is intrinsic to a spatially distributed neuron model and that special mechanisms for producing such relations need not be invoked (e.g. Carandini and Heeger 1994).

Discussion

In this paper I have shown in a variety of ways that the firing rate gain of a neuron cannot be controlled by balancing excitatory and inhibitory conductances (i.e. feedforward control). Thus, for example, the firing rate gain of an afferent input remains the same, regardless of the combination of excitatory and inhibitory conductances activated by descending inputs. The present conclusion corroborates and extends our earlier finding (Capaday and Stein 1987a) and that of Holt and Koch (1997), who have reached the same conclusion based on an analysis of the steady-state firing of a cortical neuron model. Here I have shown that this principle applies to transient and steady-state firing modes. I have also shown that this principle applies equally to linear and non-linear F/g_e, or F/I relations, as well as when synaptic inputs activate voltage dependent intrinsic conductances such as the L-type calcium conductance. Furthermore, I have systematically investigated different spatial combinations of excitation and inhibition distributed across the neuron. Firing rate gain cannot be controlled by different spatial distributions of excitation and inhibition. In this study I specifically dealt with the firing rate gain of an added excitatory input to a neuron whose firing was maintained constant despite added inhibition (Eq. 11). This point is important since the added excitatory input acts in each case on a neuron with different total membrane conductance; but despite this the change of firing rate is the same.

It was also shown, as expected, that inhibitory feedback does change a neuron's firing rate gain (Fig. 6). Thus, to the extent that the model of Carandini and Heeger (1994) incorporates true inhibitory feedback, the firing rate gain will be changed. However, it appears that inhibitory feedback will change the gain by a constant (Fig. 5), rather than as a function of the input (e.g. luminous contrast) as suggested by Carandini and Heeger (1994). Furthermore, the observation that the relation between dendritic excitation and firing rate is non-linear makes two points at once. First, linear F/g_e or F/I relations obtained from current injection at the soma are not general descriptors of a neuron's input-output properties. Second, non-linear curves relating firing rate to excitation need not be produced by combinations of excitation and inhibition as suggested by Carandini and Heeger (1994).

Why is firing rate gain independent of the particular mixture of excitatory and inhibitory conductances underlying the firing? Another way of asking the question is why does the time to fire (t_f) not change when increasing the excitatory conductance compensates the effects of an added inhibitory conductance. For the models considered here, it is not possible to obtain a closed form solution for t_f because the equations cannot be integrated. However, an intuitive understanding of the problem can be obtained by considering a simplified linear parallel conductance model in which there are three conductances, the resting conductance (g_r), a variable excitatory conductance (g_e), and a variable inhibitory conductance (g_i). The time to fire of all such models is akin to the simple RC-neuron model of Lapique (1926) and is given by:

$$t_f = -\tau_m \times \ln\left(1 - \frac{Vt}{Vss}\right) \tag{12}$$

and

$$Vss = \frac{g_r \times Vr + g_e \times Ve + g_i \times Vi}{g_r + g_e + g_i} \tag{13}$$

where $\tau_m = Cm/(g_r+g_e+g_i)$ is the membrane time constant, Cm the membrane capacitance, Vss the steady state membrane potential and Vt the firing threshold. By considering only the first term of a Taylor series expansion about Vt, Eq. 12 reduces to $t_f = \tau_m(Vt/Vss)$. With Vt constant, the firing rate ($1/t_f$) is a linear function of Vss. Clearly, if τ_m and Vss are changed in equal proportion, t_f will not change. Indeed, the compensation Eq. 11 leads to a slightly smaller Vss and a slightly smaller τ_m, resulting in a t_f that is essentially unchanged. The linearized version of Eq. 12, relating τ_m to $1/t_f$, also distills the essence of the idea that by controlling τ_m one can control the slope of the relation between excitation (i.e. Vss is proportional to net excitatory drive) and the time to fire, as suggested by Carandini and Heeger (1994). However, the flaw of the argument is that τ_m cannot be changed independently of Vss, as can be seen by considering the equations for τ_m and Vss.

The present computational demonstration that the firing rate gain is independent of the particular mixture of activated excitatory and inhibitory conductances underlying the firing is entirely in agreement with the experimental results of intracellular current injections in motoneurons (Granit et al. 1966; Granit 1972; Schwindt and Calvin 1973). These authors clearly showed that the interaction between injected excitatory currents and naturally produced synaptic inhibitory currents (i.e. activation of an antagonistic nerve) resulted in linear algebraic effects on firing rate. Granit in his review monograph (1972) wrote '*...the motoneuron adds E (excitation) and*

I (inhibition) algebraically in terms of spike frequencies'. Here it was shown that this result applies equally to the physiological case where all current flow is produced by activating conductances. In the past, the explanation for the simple translation of the *F/I* curves along the abscissa was that because of cable properties, synapses had little shunting effect visible at the soma (e.g. Rall 1977). Here, I have shown that strong shunting directly at the soma does not decrease gain (i.e. shunting inhibition, per se, is not divisive). Indeed Schwindt and Calvin (1973) concluded that '*While such conductance changes due to sustained synaptic input may produce changes in the efficacy of other inputs... only the net driving current, however applied, seems to be important in the rhythmic firing mode*.'

The question may arise, however, as to whether a sufficiently large increase in membrane conductance would affect the firing rate gain. Mathematically, based on Eq. 11, an increase in inhibitory conductance, no matter how large, can always be offset by an added excitatory conductance. Parameter values, however, must be physiologically plausible. In the model calculations I have used realistic values of excitatory and inhibitory conductances that spanned the primary (Fig. 3) and secondary (Fig. 4) range of motoneuron firing. This issue was also addressed experimentally by Granit et al. (1966) where large amounts of excitation and inhibition were used. The conclusion that firing rate gain was unchanged in the primary and secondary range remained valid, even when the largest inhibitions possible were produced.

One way to summarize the results presented here is by the following statement. The main determinants of firing rate gain in the models considered here are the conductances that regulate the interspike interval (g_{ahp}) and any other intrinsic conductance such as $g_{Ca\text{-}L}$, not the particular mixture of synaptic excitatory and inhibitory conductances driving the firing. Other currents/conductances, which exist in different combinations and proportions in different neuronal types, such as the voltage and calcium dependent I_c current, or the voltage dependent I_A current, can also determine the interspike interval (McCormick 1990) and thus the firing rate gain. It is noteworthy that neuromodulators affect intrinsic conductances, which in turn affect firing rate gain. For example, norepinephrine and acetylcholine act, at least in part, by decreasing the AHP conductance of cortical pyramidal neurons and thus increase their excitability (Nicoll 1988). In mammalian α-motoneurons, serotonin (5-HT) activates an L-type calcium conductance that is, in addition, voltage dependent (see details in Booth et al. 1997). The resulting inward current increases the slope of the *F/I* relation and thus the firing rate gain, as first noted by Schwindt and Crill (1982). This conductance can also be activated by type I metabotropic glutamate receptors (Svirskis and Hounsgaard 1998). This implies that a neurotransmitter mediating fast excitatory synaptic transmission may also indirectly activate an intrinsic depolarizing current and thus induce a gain change. However, it is not the synaptic current per se that produces the gain change, but ligand action on receptors capable of activating intrinsic neuronal conductances.

In conclusion, I suggest that a true change of firing rate gain measured experimentally will be due to: (1) the effects of neuromodulator substances acting postsynaptically on intrinsic conductances contributing to the discharge rate, (2) inhibitory feedback, or (3) presynaptic inhibition. However, for the first two cases the firing rate gain will be modified for all inputs to the neuron. In contrast, presynaptic inhibition of afferent terminals (Capaday and Stein 1987a) or, as suggested by Abbott et al. (1997), short-term depression of synaptic transmission are input-specific mechanisms for the control of firing rate gain.

Acknowledgements This work was supported by the NSERC of Canada and in part by the Canadian Institutes of Health Research. Charles Capaday is a senior research scholar of the Fond de la Recherche en Santé du Québec (FRSQ). The comments and suggestions of Drs. David Bennett, Claude Meunier and Daniel Zytnicki on a draft of the manuscript are gratefully acknowledged.

References

Abbott LF, Varela JA, Sen K, Nelson SB (1997) Synaptic depression and cortical gain control. Science 275:220–224

Barrett EF, Barret JN, Crill WE (1980) Voltage sensitive outward currents in cat motoneurons. J Physiol (Lond) 304:251–276

Bastian J (1986a) Gain control in the electrosensory system mediated by descending inputs to the electrosensory lateral line lobe. J Neurosci 6:553–562

Bastian J (1986b) Gain control in the electrosensory system: a role for the descending projections to the electrosensory lateral line lobe. J Comp Physiol 158:505–515

Bastian J, Courtright J (1991) Morphological correlates of pyramidal cell adaptation rate in the electrosensory lateral line lobe of weakly electric fish. J Comp Physiol 168:393–407

Bennett DJ, Hultborn H, Fedirchuk B, Gorassini M (1998) Synaptic activation of plateaus in hindlimb motoneurons of decerebrate cats. J Neurophysiol 80:2023–2037

Booth V, Rinzel J, Kiehn O (1997) Compartmental model of vertebrate motoneurons for Ca^{2+}-dependent spiking and plateau potentials under pharmacological treatment. J Neurophysiol 78:3371–3385

Capaday C, Stein RB (1986) Amplitude modulation of the soleus H-reflex in the human during walking and standing. J Neurosci 6:1308–1313

Capaday C, Stein RB (1987a) A method for simulating the reflex output of a motoneuron pool. J Neurosci Methods 21:91–104

Capaday C, Stein RB (1987b) Difference in the amplitude of the soleus H-reflex during walking and running. J Physiol (Lond) 392:513–522

Capaday C, Stein RB (1989) The effects of postsynaptic inhibition on the monosynaptic reflex of the cat at different levels of motor activity. Exp Brain Res 77:577–584

Carandini M, Heeger DJ (1994) Summation and division by neurons in primate visual cortex. Science 264:1333–1336

Crenna P, Frigo C (1987) Excitability of the soleus H-reflex during walking and stepping in man. Exp Brain Res 66:607–616

Granit R (1972) Mechanisms regulating the discharge of motoneurons. Liverpool University Press, Liverpool

Granit R, Kernel D, Lamarre Y (1966) Algebraic summation in synaptic activation of motoneurons firing within the 'primary range' to injected currents. J Physiol (Lond) 187:379–399

Heckman CJ (1994) Computer simulation of the effects of different synaptic input systems on the steady-state input-output structure of the motoneuron pool. J Neurophysiol 71:1727–1739

Henneman E, Mendell LM (1981) Functional organization of motoneuron pool and its inputs. In: Brooks VB (ed) Handbook of physiology, sect I: The nervous system, vol II, part I. American Physiological Society, Bethesda, pp 423–507

Holt GR, Koch C (1997) Shunting inhibition does not have a divisive effect on firing rates. Neural Comput 9:1001–1013

Hounsgaard J, Kiehn O (1993) Calcium spikes and calcium plateaux evoked by differential polarization in dendrites of turtle motoneurons in vitro. J Physiol (Lond) 468:245–259

Jack JJB, Noble D, Tsien RW (1975) Electric current flow in excitable cells. Oxford University Press, Oxford

Johnston D, Wu SM-S (1995) Foundations of cellular neurophysiology. MIT Press, Cambridge

Kernel D (1965) High-frequency repetitive firing in cat lumbosacral motoneurons stimulated by long-lasting injected currents. Acta Physiol Scand 65:74–86

Kiehn O (1991) Plateau potentials and active integration in the 'final common pathway' for motor behaviour. Trends Neurosci 14:68–73

Lapique L (1926) Excitabilité en fonction du temps. Presse Universitaires de Paris, Paris

Lee RH, Heckman CJ (1996) Influence of voltage-sensitive dendritic conductances on bistable firing and effective synaptic current in cat spinal motoneurons in vivo. J Neurophysiol 76: 2107–2110

MacGregor RJ (1987) Neural and brain modeling. Academic Press, New York

Matthews PBC (1999) The effect of firing on the excitability of a model motoneurone and its implications for cortical stimulation. J Physiol (Lond) 518:867–882

McCormick DA (1990) Membrane properties and neurotransmitter actions. In: Sheperd GM (ed) The synaptic organization of the brain. Oxford University Press, Oxford, pp 32–66

Nelson ME (1994) A mechanism for neuronal gain control by descending pathways. Neural Comput 6:242–254

Nicoll R (1988) The coupling of neurotransmitter receptors to ion channels in the brain. Science 241:545–551

Powers RK (1993) A variable-threshold motoneuron model that incorporates time and voltage-dependent potassium and calcium conductances. J Neurophysiol 70:246–262

Rall W (1977) Core conductor theory and cable properties of neurons. In: Kandel ER (ed) Handbook of physiology, the nervous system: cellular biology of neurons, vol I, part I. American Physiological Society, Bethesda, pp 39–97

Schwindt PC, Calvin WH (1972a) Membrane-potential trajectories between spikes underlying motoneuron rhythmic firing. J Neurophysiol 35:311–325

Schwindt PC, Calvin WH (1973) Equivalence of synaptic and injected current in determining the membrane potential trajectory during motoneuron rhythmic firing. Brain Res 59:389–394

Schwindt PC, Crill WE (1982) Factors influencing motoneuron rhythmic firing: results from a voltage-clamp study. J Neurophysiol 48:875–890

Shapovalov AI (1972) Extrapyramidal monosynaptic and disynaptic control of mammalian alpha-motoneurons. Brain Res 40:105–115

Svirskis G, Hounsgaard J (1998) Transmitter regulation of plateau properties in turtle motoneurons. J Neurophysiol 79:45–50

Xing J, Gerstein G (1996) Networks with lateral connectivity. I. Dynamic properties mediated by the balance of intrinsic excitation and inhibition. J Neurophysiol 75:184–199